

Capacitance Characterization Methods and Ageing Behaviour of Supercapacitors

P. KURZWEIL¹ and B. FRENZEL

¹⁾ University of Applied Sciences, Kaiser-Wilhelm-Ring 23, D-92224 Amberg, Germany

R. GALLAY²

²⁾ Maxwell Technologies, CH-1728 Rossens, Switzerland

Abstract. Commercial MAXWELL capacitors were investigated by *ac* impedance spectroscopy, chronoamperometry, constant current discharge and other transient techniques in order to determine rated capacitances reliably. Capacitance is outlined as a dynamic quantity that depends on the voltage and the state of charge of the supercapacitor. Capacitance is divided up in a double-layer capacitance at the “outer” electrode surface and a pseudocapacitance due to slow electrochemical processes depending on voltage: $C = C_0 + kU$. Rated capacitance is determined as the differential capacitance at 50% or 75% of the rated voltage U_0 , advantageously.

The University of Applied Sciences in Amberg is situated not far from Nuremberg in the south-west of Germany. Since the 1990s, manifold R & D activities have been carried out in the field of supercapacitors in tight cooperation with HYDRA/AEG [1], DORNIER/DAIMLERCHRYSLER [2], and MAXWELL.

1 Capacitance: a linear function of voltage

Capacitance, electric charge and energy of a bipolar supercapacitor were studied as functions of voltage. The investigation was based on discharge characteristics presented in the 1997 seminar [3]. At that time, we demonstrated the impressive power and efficiency of a 30 V/65 F supercapacitor by starting a Mercedes C220 on a spring morning at an ambient temperature of 12 °C. The battery was completely disconnected from the starter, and the supercapacitor in Figure 1 replaced the battery completely. The transients of capacitor current and voltage were recorded during cranking by help of an oscilloscope. The mean values of power and energy were calculated as functions of instantaneous current and voltage.

During cranking an almost constant electric power of 1 kW was measured. A single start required an electric charge of 150 As and a minimum capacitance of 33 F. ΔU dropped to 4.5 V depending on the operating voltage of the starter (12–18 V).

According to the recommendations of EUCAR [4] – an European association of DAIMLERCHRYSLER, Fiat, Opel, PSA, Renault, Rover, Volkswagen, and Volvo – capacitance was determined by help of the voltage drop ΔU from 60% to 40% of the rated voltage (see Fig. 2).



Fig. 1: Starting a Mercedes C220 with a 30 V/65 F supercapacitor (bipolar metal oxide technology, 4 Wh/l, 1.3 Wh/kg).

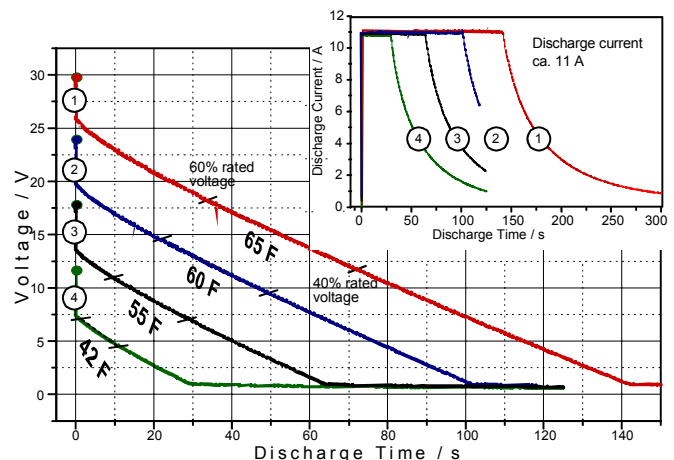


Fig. 2: Constant current discharge characteristics of the supercapacitor at different operating voltages (states of charge).

For capacitance determination, EUCAR recommends a discharge current of 5 mA/F (single cell). Thus:

$$0.005 \text{ A/F} \cdot 30 \text{ cells} \cdot 65 \text{ F} \approx 10 \text{ A}$$

Capacitance determined by discharge characteristics strongly depends on the discharge current and the voltage (state of charge) of the capacitor.

Electric charge and energy in Figure 3 were calculated by numerical integration of the total discharge characteristics with respect to time (see Figure 4).

- At constant discharge currents (12, 25, 50, 100 A) electric charge depends on the applied voltage. This is consistent with the fact that the electric charge should be the product of capacitance and voltage. However, C depends on U .

$$Q(U) = \int_0^{\Delta t} I(t) dt = C(U) \cdot U$$

- The mean least squares fit curve over all the measurements at 25, 50 and 100 A shows that integral capacitance depends linearly on the applied voltage.

$$C(U) = \frac{Q(U)}{U} = C_0 + k \cdot U \approx 60 \text{ F} + 0.14 \text{ F} \cdot U$$

Capacitance seems to be an approximately linear function of voltage: $C(U) = C_0 + k \cdot U$, whereby C_0 is the capacitance at 0 V.

As we will outline in section 2.3, capacitance calculated by $C = \Delta Q / \Delta U = I \Delta t / \Delta U$ in the given voltage window $\Delta U = (0.6 - 0.4) \cdot U_0$ at constant current I strongly depends on whether the slope $\Delta U / \Delta t$ was determined accurately. The value of this differential capacitance may be smaller or larger than the integral capacitance of the total discharge characteristics $C = \int I dt / \Delta U$.

- The available energy approximately shows the expected squared dependence on voltage: $W \approx \frac{1}{2} \cdot 60 \text{ F} \cdot U^2$.

Understanding $C(U)$ as a function of voltage, we get:

$$I = \frac{dQ}{dt} = \frac{d(C(U)U)}{dt} = \frac{d[(C_0 + kU)U]}{dt} = (C_0 + 2kU) \frac{dU}{dt}$$

$$C(U) = \frac{Q}{\Delta U} = \frac{1}{\Delta U} \int_0^{\Delta U} (C_0 + 2kU) dU = C_0 + k \Delta U$$

$$\begin{aligned} W &= \int_0^{\Delta t} U(t) \cdot I(t) dt = \int U dQ = \int U d[C(U)U] \\ &= \int U(C_0 + 2kU) dU = \frac{1}{2} C_0 U^2 + \frac{2}{3} k U^3 \end{aligned}$$

The notion of capacitance is well understood when it is constant in the voltage domain. In the case of a voltage linear dependency, a clear difference must be done

- between the C -coefficient in the relation linking the current amplitude and the voltage time variation and
- the C -coefficient linking the charge and the voltage.

What we are used to call the capacitance is in the constant case the C -coefficient which is equal for both relations. This insight is verified in the following.

Tab. 1: Differential capacitance of the supercapacitor in Figure 1 determined by constant current discharge at different applied volages (see Figure 2).

$C = \frac{dQ}{dU} = I \frac{dt}{dU} = \frac{I \cdot (t_2 - t_1)}{U_1 - U_2} \quad (0.6 \dots 0.4 \cdot U_0)$						
U_1	I	Δt	Q	ΔU	dU/dt	C
V	A	s	As	V	V/s	F
12	10.8	9.3	101	2.4	0.253	42
18	10.9	17	186	3.4	0.200	55
24	11.0	26	286	4.7	0.182	60
30	11.0	35	387	5.9	0.169	65

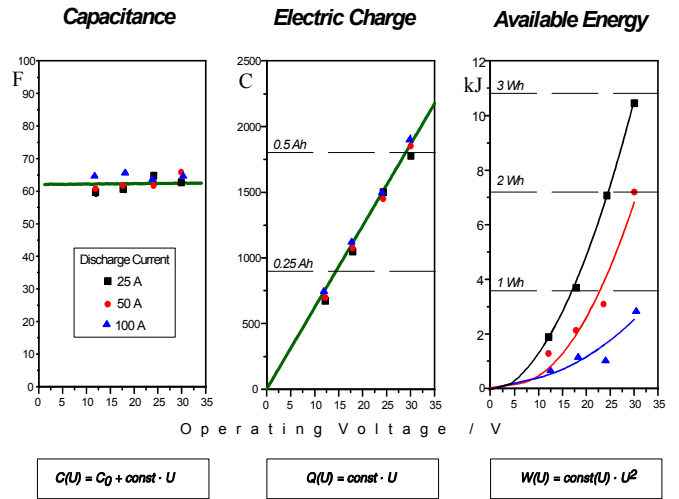


Fig. 3: Integral capacitance, electric charge and available energy of a 30 V/65 F supercapacitor at different discharge currents and voltages. Data from integration method.

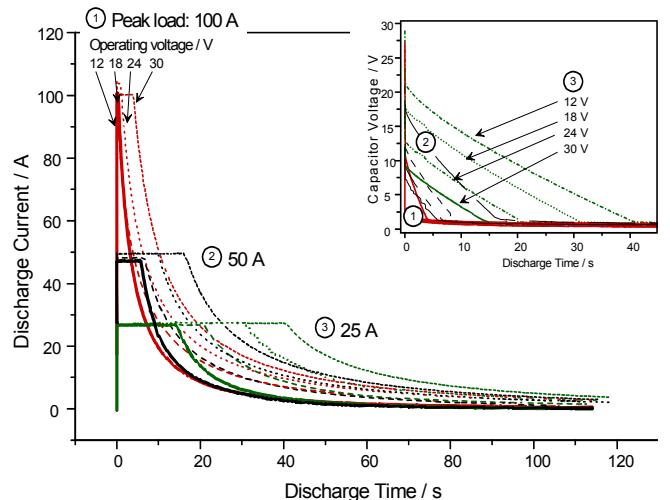


Fig. 4: Discharge characteristics at different voltages and currents, which lead to the results in Figure 3.

2 How capacitance depends on voltage and state-of-charge

2.1 Which rated capacitance is correct?

This section deals with feasible methods for industrial quality assurance during the fabrication of supercapacitors. As capacitance depends on voltage – see section 1 – it does not astonish that diverse transient techniques yield different results (Figure 5).

- *ac* impedance spectroscopy and cyclic voltammetry provide differential capacitances which depend on voltage. The integral average value – or the differential capacitance at one half of the rated voltage – we consider to be one of the most accurate and reliable value that can be given for the rated capacitance of a commercial supercapacitor.
- The simple method described in IEC 40/1378 [8], by which the linear drop of the rated voltage from 80% to 40% is evaluated, provides the highest capacitance values of all methods.

The molecules at the electrochemical interface between electrode and electrolyte show a nonlinear response to the electric field. Capacitive and Faradaic charges coexist. This charge, divided by the potential range from which it is transferred, constitutes a *pseudocapacitance* since it is not associated with a purely capacitive phenomenon. Transient techniques, which generate fast voltage changes, reflect the fast charge/discharge processes with “frozen” diffusion at the outer electrode surface. At slow voltage changes the slow electrode reactions in the inner electrode surface (strongly depending on voltage) additionally contribute to the measured capacitance values (see Figure 6 and the following sections).

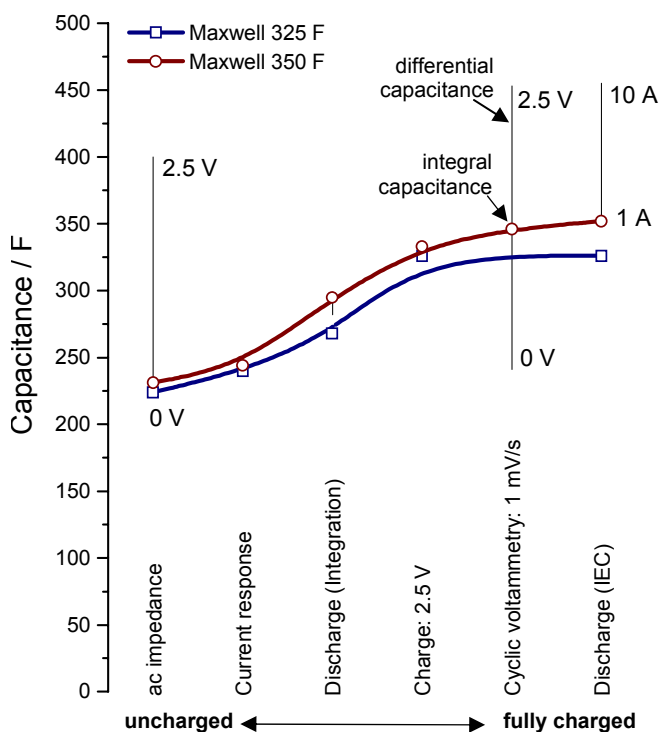
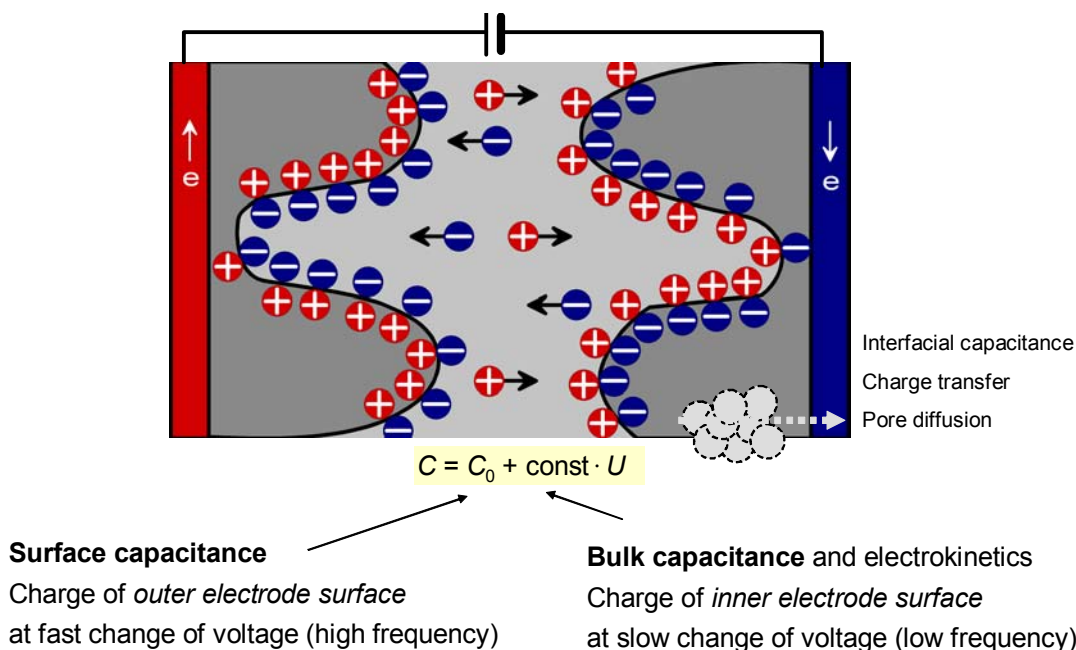


Fig. 5: Capacitance of Maxwell capacitors (BCAP0350) determined by different measuring techniques, which cause a different state-of-charge of the capacitor.

Fig. 6: Model for the capacitance of a supercapacitor due to the double-layer C_0 and faradic reactions $C(U)$.



2.2 Capacitance: a mirror of electrokinetics

In Fig. 7/8 the frequency response of capacitance of a Panasonic “GoldCap” [5] and a Maxwell “BCAP0350” are shown at different *dc* voltages applied by a potentiostat. Both capacitors show qualitatively the same dependence on voltage, although the electrolytes are based on propylene carbonate and acetonitrile, respectively. The electrodes consist of active carbon in both cases, but the preparation method is different.

The capacitance values found both by impedance spectroscopy and by integration of the discharge characteristics are in good agreement.

The frequency response of differential capacitance reflects the different time domains of fast surface charging and slow faradic reactions in the “inner” surface of the porous electrodes [7, 10]. Capacitance at high frequencies – caused by the dielectric properties of the electrode/electrolyte interface – does not depend on voltage. But capacitance at low frequencies is determined by the overvoltage of the kinetically inhibited charge transfer and mass transport processes.

We define **rated capacitance** C_n at 75% of the rated *dc* voltage U_0 (for *ac* impedance, Fig. 7) or $50\% \cdot U_0$ (transient techniques, Fig. 10), respectively.

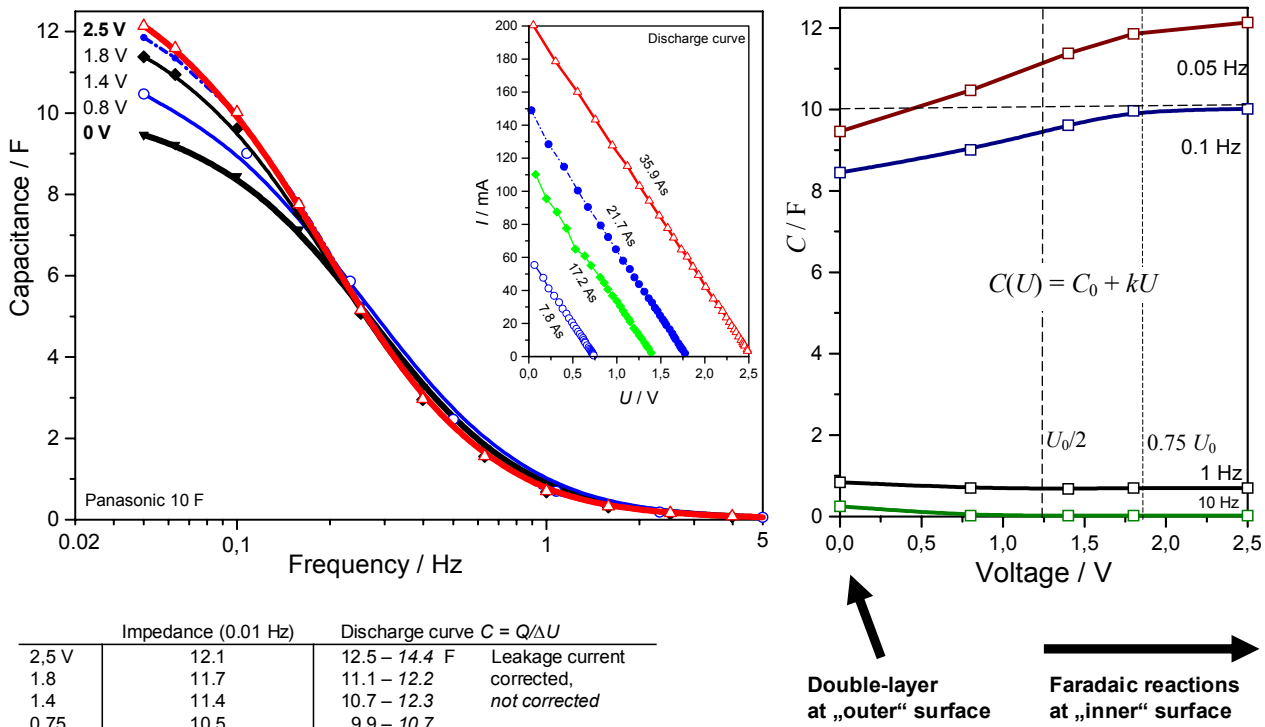


Fig. 7: Frequency response of capacitance of a PANASONIC 10 F/2.5 V-supercapacitor at different voltages.

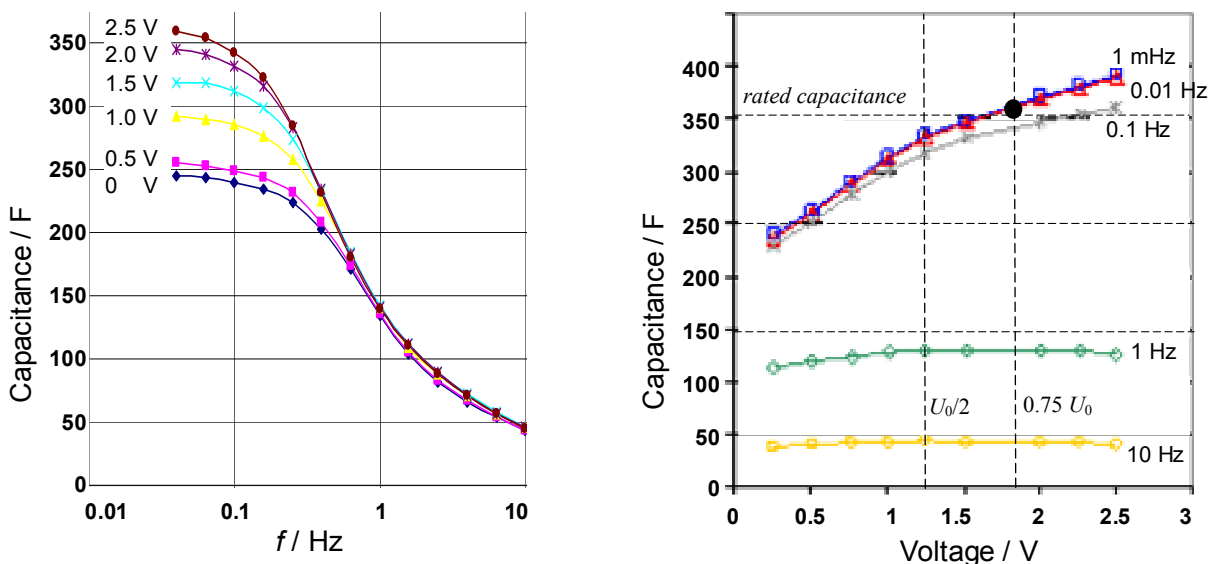


Fig. 8: Frequency response of differential capacitance of a Maxwell BCAP0350 capacitor (left: data from [12], right: [13]).

2.3 Integral and differential capacitance

The approximately linear dependence of capacitance on voltage $C(U) = C_0 + k \cdot U$ can be understood by help of the cyclic voltammogram. A supercapacitor may have a differential capacitance dQ/dU (at some voltage), with a corresponding medium integral capacitance $Q/\Delta U$ (in some wide voltage window).

By help of electric charge, we describe the pseudo-capacitance of a supercapacitor as a differential quantity which depends on the scan rate v of voltage.

- Electric charge (in Figure 9)

$$Q = \int_0^{\Delta t} I(t) dt = \frac{1}{v} \underbrace{\int_0^{\Delta U} I(U) dU}_{\text{Area}} \quad \text{and} \quad v = \frac{dU}{dt}$$

- Integral capacitance: mean of differential capacitance

$$\bar{C} = \frac{Q}{\Delta U} = \frac{1}{\Delta U} \int_0^{\Delta U} C(U) \cdot dU = C(U_0/2)$$

- Differential capacitance at $v = \text{const}$ (in Figure 10)

$$C(U) = \frac{dQ}{dU} = \frac{I(U)}{v} \quad \text{and} \quad I = \frac{dQ}{dt} = C \frac{dU}{dt} = C \cdot v$$

- Available energy

$$W = \int_0^{\Delta t} U(t) \cdot I(t) dt = \int_{U_1}^{U_2} Q dU = \int_{U_1}^{U_2} C(U) \cdot U dU$$

If C were constant only, it holds: $W = \frac{1}{2} C(U_2^2 - U_1^2)$

The extremely broad current peaks in Figure 9 reveal the heterogeneity of the electrode surface. Current and electric charge are qualitatively related to the penetration depth of the signal (concentration wave) into the porous electrode materials [6, 7].

a) Low scan rates reflect the behaviour of the capacitor in the dc case: $I \sim \sqrt{v}$ and $Q \sim v^{-1/2}$ due to slow diffusion controlled processes, when the “inner” surface is accessed by the electroactive ions from the electrolyte. In Figure 9 electric charge equals

$$Q(v) = 332 \text{ C} + 15 (v \text{ in mV/s})^{-1/2} \quad (\text{fit quality } 93\%)$$

b) At high scan rates v current and sweep rate are proportional: $I \sim v$ and $Q \sim v^{-1}$. Voltammetric charge shows “frozen” diffusion. Fast electrode reactions determine the capacitance at the “outer” surface.

2.4 Practical benefit for capacitor fabrication

Timesaving techniques of capacitance measurement are required for industrial quality control. The quasi-linear relationship in Figure 10 is useful to determine rated capacitances by measurements at lower test voltages – which require less time for charging.

$$\frac{\text{Rated } C}{\text{Test } C(0.5 \text{ V})} = \frac{241 \text{ F} + 85 \text{ F/V} \cdot 1.25 \text{ V}}{241 \text{ F} + 85 \text{ F/V} \cdot 0.5 \text{ V}} = \frac{347 \text{ F}}{326 \text{ F}} = 1.064$$

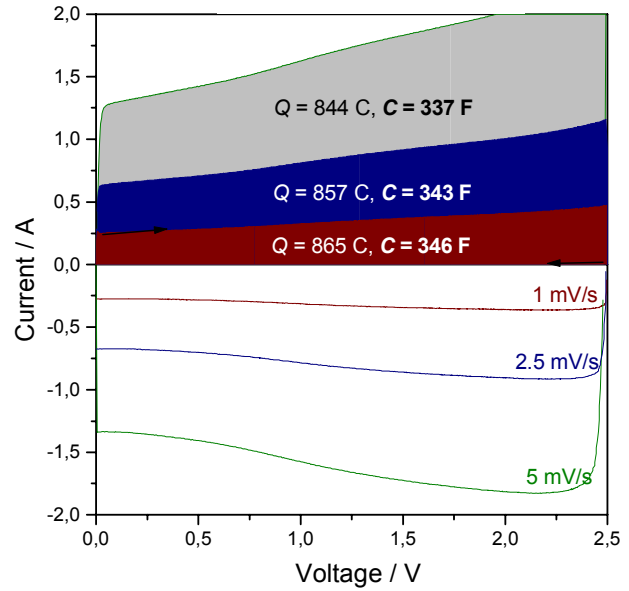


Fig. 9: Determination of integral capacitance of a MAXWELL supercapacitor (350 F, 2.5 V) by cyclic voltammetry.

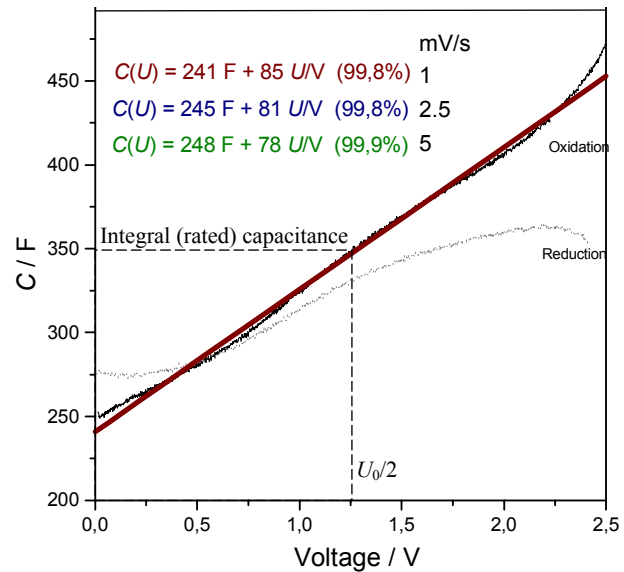


Fig. 10: Differential capacitance of a MAXWELL supercapacitor BCAP0350 (350 F, 2.5 V) at different scan rates

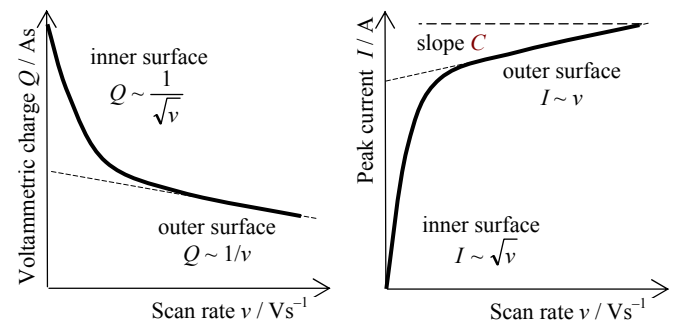


Fig. 11: Voltammetric charge in a given voltage window (left) and peak current at a given voltage (right) depend on the scan rate of voltage [7].

3 Constant current discharge at rated voltage

3.1 Discharge according to IEC 40/1378

The easy method in Figure 12 according to the IEC 40/1378 standard [8] provides a more or less correct estimation of the actual capacitance of a supercapacitor. The supercapacitor is fully charged at its rated *dc* voltage for 24 hours. Then, the power source is cut off, and the capacitor is discharged by help of an electronic load at a constant current of about 5 mA/F.

- *Capacitance* is measured by help of the period of time t_2-t_1 , during which the voltage across the capacitor declines from 80 % to 40 % of the applied voltage U_0 . At high currents, the linear voltage region in the discharge characteristics becomes smaller and smaller, and the error of the capacitance calculated by $C = I \Delta t / \Delta U$ increases dramatically. The linear relation of differential capacitance and current $I = C \, dU/dt$ holds for capacitors with low internal resistance. Table 2 compiles the theoretical corrections for equivalent circuits which take account of the series resistance R_1 (electrolyte resistance) and the *dc* leakage resistance R_2 (polarization resistance in parallel) in real supercapacitors.
- *Internal resistance*. The voltage drop $\Delta U_R = IR$ is determined as the point of intersection between the linearly extrapolated voltage curve and the time axis immediately after closing the discharge circuit.

- *Electric power* reflects the maximum current the supercapacitor is able to supply, when it is discharged to the half of its rated voltage.

$$P = \left(\frac{80\% + 40\%}{2} \right) U_0 I = 0.6 \cdot U_0 I = 0.6 \cdot U_0 \cdot \frac{\Delta U_R}{R}$$

3.2 Integration of the discharge curve

Exact measurements require to integrate the current flowing through the capacitor with respect to time (Figure 13). The correction of leakage currents $I(t \rightarrow \infty)$ may be neglected in most cases.

The higher the discharge current, the higher is the capacitance. Moreover, capacitance depends on the discharge time, until a constant value is reached. At operating voltages lower than the rated voltage of 2.5 V, smaller capacitance values result.

The discharge method captures capacitance at a certain voltage and state-of-charge – i. e. capacitance comprises the “outer” double-layer capacitance of the electrode/electrolyt interface and the “inner” pseudo-capacitance of the slow, diffusion controlled faradaic reactions in the electrode pores. Thus, in the electric field at 2,5 V a higher capacitance is observed than at 1,5 V. Capacitance shows the linear dependence on voltage $C(U) = C_0 + \text{const} \cdot U$ as mentioned above (see also [9] for capacitors of different manufacturers). Therefore, capacitance strongly depends on the voltage window which is passed during discharge.

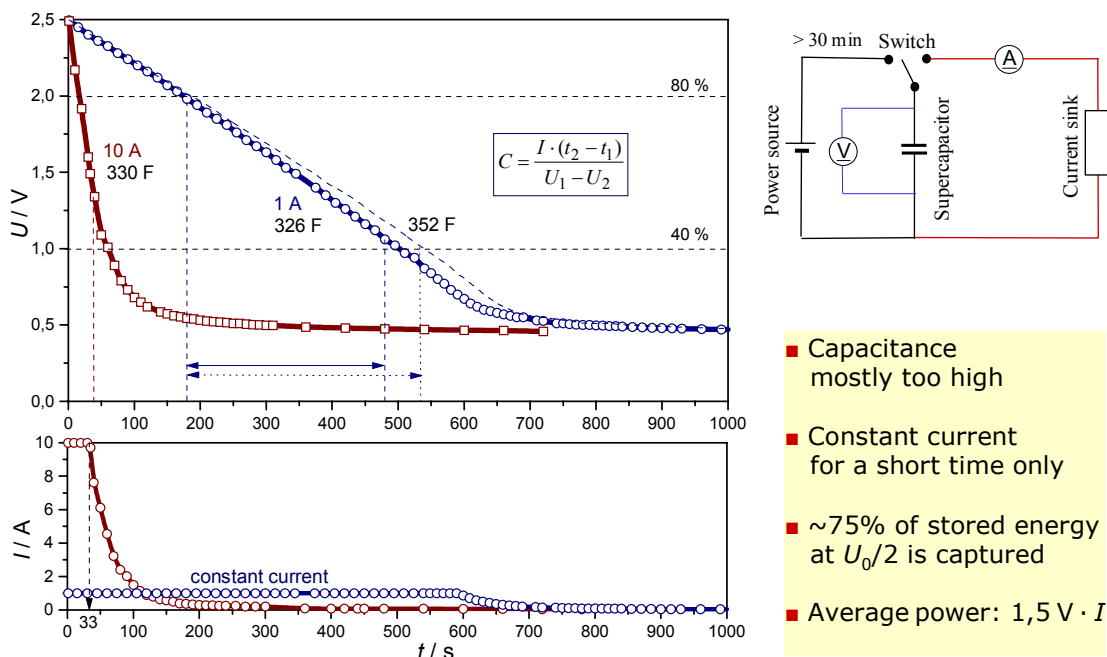
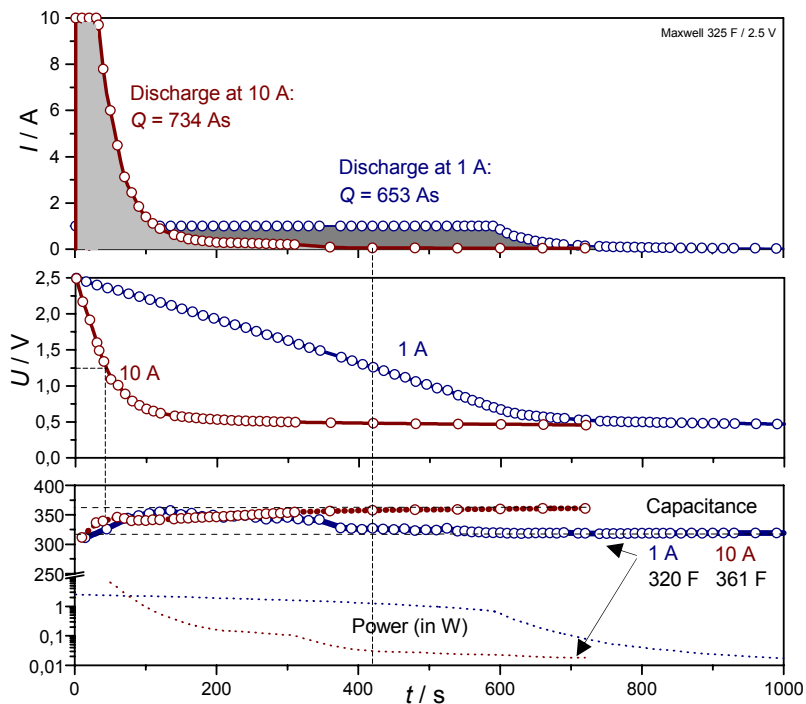


Fig. 12: IEC 40/1378: Discharge characteristics of MAXWELL BCAP 325 F and 350 F (dahed line) at different currents



- Electric charge

$$Q(t) = \int I(t) dt$$
- Capacitance ($R \rightarrow 0$)

$$C(t) = \frac{Q(t)}{U_0 - U(t)}$$
- Peak power at $U_0/2$

$$P_{\max} = \frac{U_0^2}{4R_1}$$

Fig. 13: Determination of capacitance by integration of the discharge characteristics (MAXWELL BCAP, 325 F). Dashed lines: The capacitance values reached at half of the rated voltage read 327 F (at 1 A) and 337 F (at 10 A). The internal resistance may be neglected ($R \approx 0.002 \Omega$, see Figure 15, causes an error of $\Delta C < 1 \text{ F}$ at $U < 1.25 \text{ V}$).

Tab 2. Theoretical response of linear networks

Model of the capacitor	Voltage step (Chronoamperometry)	Current step (Chronovoltametry)	Linear voltage sweep (Voltamperometry) and constant current discharge
a)	If a perturbation signal were applied to a capacitor, its answer function is obtained by LAPLACE transformation of the transfer function $\underline{Z}(p) = [pC_1]^{-1} = \underline{U}(p)/\underline{I}(p)$, whereby $p = j\omega$.		
	$\underline{I}(p) = \frac{\underline{U}(p)}{\underline{Z}(p)} = \frac{U_0}{p} : \frac{1}{pC_1} = U_0 C$ $\Rightarrow I(t) = U_0 C \delta(t)$	$\underline{U}(p) = \underline{Z}(p) \cdot \underline{I}(p) = \frac{I_0}{p^2 C}$ $U(t) = \frac{I_0 t}{C}$	$\underline{I}(p) = \frac{\underline{U}(p)}{\underline{Z}(p)} = \frac{v}{p^2} : \frac{1}{pC} = \frac{vC}{p}$ $I(t) = C v = C \frac{dU}{dt}$
b)	LAPLACE transformation of the transfer function $\underline{Z}(p) = R_1 + [pC_1]^{-1} = \underline{U}(p)/\underline{I}(p)$		
<p>$\tau = R_1 C_1$</p>	$I(t) = \frac{U_0}{R_1} \cdot e^{-t/\tau}$	$U(t) = \frac{I_0 t}{C} + R_1 I_0$	$I(t) = C v \cdot [1 - e^{-t/\tau}]$
c)	LAPLACE transformation of the transfer function $\underline{Z}(p) = \frac{\underline{U}(p)}{\underline{I}(p)} = R_1 + \frac{1}{pC_1 + 1/R_2} = \frac{R_1 + R_2 + pR_1 R_2 C}{1 + pR_2 C}$		
<p>$\tau = \frac{R_1 R_2 C}{R_1 + R_2}$</p>	$I(t) = \frac{U_0}{R_1 + R_2} \left[1 + \frac{R_2}{R_1} e^{-t/\tau} \right]$ <p>and $I(t=0) = 0$</p>	$U(t) = R_1 I_0 + R_2 I_0 [1 - e^{-t/\tau}]$	$I(t) = \frac{v R_2 C}{R_1 + R_2} \left\{ 1 - e^{-t/\tau} + \frac{R_1}{R_1 + R_2} \left[e^{-t/\tau} + \frac{t}{\tau} - 1 \right] \right\}$

4 Chronoamperometry for industrial use

We present *Chronoamperometry (current response after a voltage step)* as a simple method to determine the rated capacitance of supercapacitors in industrial quality control within a few seconds.

Before the measurement, the capacitor terminations are short-circuited for at least 30 minutes. The rated voltage is applied and the current response – measured as voltage drop across a shunt – is recorded using an oscilloscope.

As the total current flows across C at the beginning of charging ($t \rightarrow 0$), R_2 can be neglected in circuit c) in Table 2. R_2 has no effect on the initial slope of current dI/dt . Capacitance in circuit b) after the voltage step reads:

$$\lim_{t \rightarrow 0^+} \frac{dI}{dt} = -\frac{U_0}{R_1^2 C} \quad \Rightarrow$$

$$C = -\frac{U_0}{R_1^2 \cdot \left. \frac{dI}{dt} \right|_{t=0}} \quad \text{wherein} \quad R_1 = \frac{U_0}{I(t=0)}$$

R_1 sum of standard resistor (shunt), contact resistances and series resistance of the capacitor

R_2 internal parallel resistance of the supercapacitor

We used a power source (GOSSEN SSP 62 N) with current limitation switched off, and a 0,1 Ω standard resistor of high quality (BURSTER).

With switching on the power source at the point of time $t = 0$, the applied voltage jumps from 0 V to $U_0 = 2,5$ V. A current peak occurs, followed by an approximately linear decrease of current dI/dt within about 3 seconds. At longer times, the charge curve shows an exponential decay (see Figure 14).

The experimental setup allows swift reiterations of the measurements. The error (standard deviation) of 15 single measurements is given Table 3. The series resistance of the capacitor including contact resistance was about 0.02 Ω .

Chronoamperometry – just as *ac* impedance spectroscopy at frequencies above 0.1 Hz – reflects the double layer capacitance C_0 of the uncharged capacitor without the slow faradic reactions controlled by pore diffusion.

The linear function $C(U) = C_0 + k \cdot U$ in Fig. 10, which is once determined for the prototype of a series of commercial supercapacitors, allows to extrapolate the C_0 value for usual rated voltages (see section 2.4).

Tab. 3: Maxwell BCAP capacitors: time window $\Delta t = 3$ s.

Capacitor	R_1 / Ω	dI/dt in A/s	C / F	Error	
				ΔC	in %
BCAP325	0,12	-0,7	237	$\pm 1,3$	$\pm 0,53$ %
BCAP350	0,12	-0,7	252	$\pm 1,6$	$\pm 0,63$ %

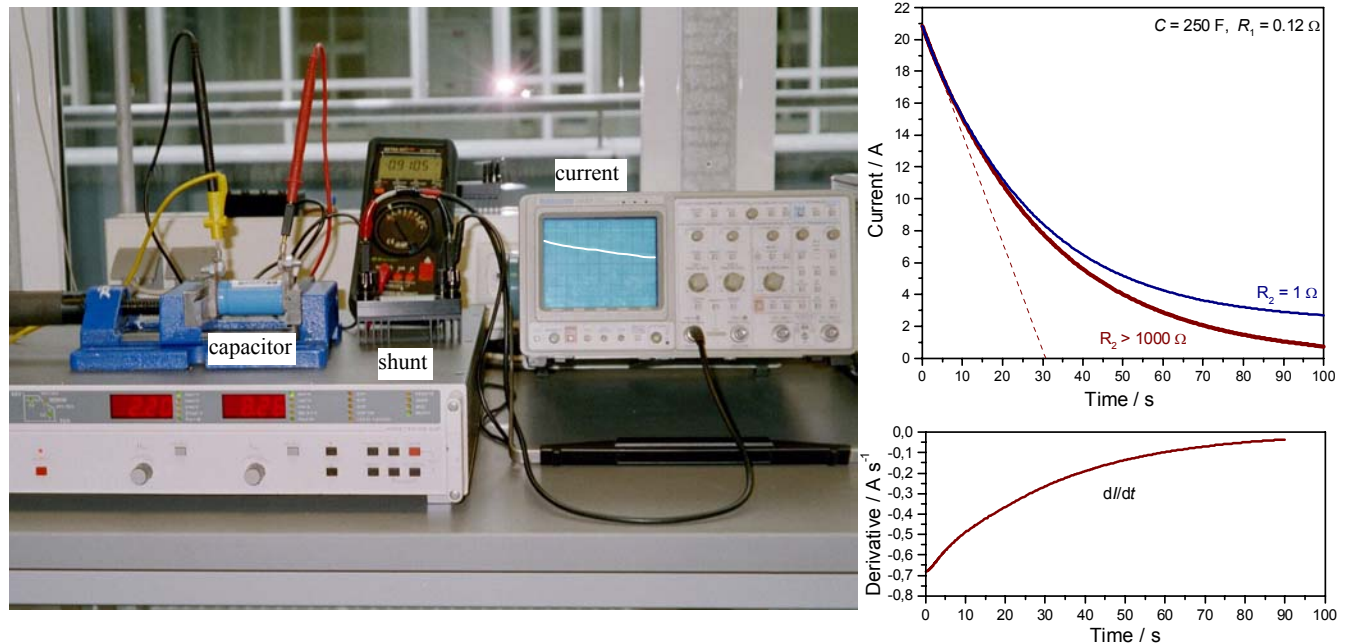


Fig. 14.: Left: Experimental setup for chronoamperometry (left). Right: Calculated current decay after a voltage step of 2.5 V, whereby the internal resistance R_2 in the circuit in Table 2 c) is varied between leakage (1 Ω) and isolation (1000 Ω).

5 Ageing of supercapacitors

5.1 *ac* Impedance Spectroscopy: the effect of a heat treatment

In the ageing test MAXWELL supercapacitors (BCAP0350) were charged at a constant voltage of 2.5 V and at an ambient temperature of 70 °C for 1000 hours. Figure 15 shows that the increase of resistance is more pronounced than the deterioration of capacitance.

a) Internal **resistance** increases by a factor of 3 to 4.5 during the thermal treatment at 70°C for 1000 h. The changes equal some milliohms and contain contact resistances. In the diagram of capacitance versus resistance (Fig. 15 a) useful capacitance and internal resistance (ESR) can directly be read.

b) **Capacitance** does not significantly change in 1000 hours at 70°C. We know from further investigations that capacitance rather gets better than worse by storing the capacitor at elevated temperatures. In Figure 15 a) capacitance was corrected by the electrolyte resistance R_s to show the actually efficient capacitance of 232 ± 2 F before and after the heat treatment. This corresponds to C in the equivalent circuit in Table 2 c).

c) Maximum **reactive power** – as a relative measure of the maximum capacitance the capacitor can supply – decreases from 417 var to 192 var. This corresponds to a theoretical decline of interfacial capacitance by 7% from 106 F to 98 F (see below).

5.2 The nature of the ageing process: analysis of the impedance spectra

It is noteworthy that the impedance spectra before and after the heat treatment are nearly congruent, except a shift of resistance (see Figure 16).

The change of resistance seems typical for an “electrical” ageing process caused by the growth of isolating interlayers or gas bubbles. On the other side, the moderate decline of capacitance reflects the stability of the electrode/electrolyte interface.

Furthermore, the maximum reactive power is reached at higher frequencies than the maximum of capacitance (see Figure 15 a and c). This may be a hint that ageing processes in the “outer” surface cause the deterioration of capacitance.

In literature supercapacitors are often modelled by a RC series combination of a resistance R_s and a equivalent series capacitance C_s . (which implies that the *dc* resistance R_2 is infinitely high)

$$\text{Im } \underline{Z} = |\underline{Z}| \sin \varphi \quad \Rightarrow \quad C_s = \frac{-1}{2\pi f \cdot \text{Im } \underline{Z}}$$

We stressed in the last year seminar [10] that the “leakage resistance” R_2 – due to the charge transfer and faradaic reactions in the porous electrodes – cannot be neglected, because supercapacitors show considerable leakage currents and self discharge. Therefore, capacitance must be written in a parallel equivalent circuit (see Table 2 c, whereby $R_1 < 10$ mΩ may be neglected) or a more complicated equivalent circuit (see Figure 15). At low frequencies only, there is no difference between the parallel capacitance $C = \text{Im } \underline{Y}/\omega$ and the series capacitance model $C = -[\omega \text{Im } \underline{Z}]^{-1}$.

Furthermore, the mass transfer impedance – due to the diffusion and absorption of ions from the electrolyte at the porous electrodes – cannot be neglected. The current through a supercapacitor with the equivalent circuit in Figure 16 reads:

$$I = C_1 \frac{dU}{dt} + I_{\text{faradic}} = \frac{U_{\text{pore}}}{R_{\text{pore}}}$$

DELEVIE [11] solved this equation for a one-dimensional pore of the length l . Its impedance reads [6]:

$$\underline{Z}(j\omega) = \frac{1}{j\omega C_1 + \frac{1}{\underline{Z}_{\text{faradic}}}} = \frac{a \coth \sqrt{l^2 b}}{\sqrt{b}}$$

Herein a is a constant depending on the electrolyte resistance R_1 , the surface roughness S/A . Constant b additionally comprises the double-layer C_1 and absorption capacitance C_2 , and the charge transfer resistance R_2 . C_2 and R_2 are combined in $\underline{Z}_{\text{faradic}}$.

$$a = \frac{R_1 S}{l A} \quad \text{and} \quad b = \frac{a S}{l} \left(j\omega C_1 + \frac{1}{\underline{Z}_{\text{faradic}}} \right)$$

Figure 16 shows how thick porous layers reduce the slope of the low-frequency straight line and increase the charge transfer arc. The striking high-frequent quarter circle, and the low-frequency 45° slope in the complex plane plot occur with increasing surface roughness and electrolyte resistance (constant a). We conclude:

A heat treatment at 70 °C for 1000 hours does not destroy the active mass of the capacitor. The ageing process is dominated by “electrical” factors more than by electrochemical reactions. Reasons for the ageing may be traces of water and absorbed gases in the electrolyte and the electrodes [9].

The Swiss PSI institute [12] predicts estimated lifetimes of far more than ten years for supercapacitors based on carbon and acetonitrile. The speed of capacitance degradation is roughly doubled by a) a temperature increase of 10 °C (above 20 °C) or b) a voltage increase of 0.1 V (above 2,5 V). The estimated lifetime at 70°C would be 8.5 to 12.5 times shorter than the hypothetical lifetime of 200 years – consequently, the capacitor would work for 16 to 23 years.

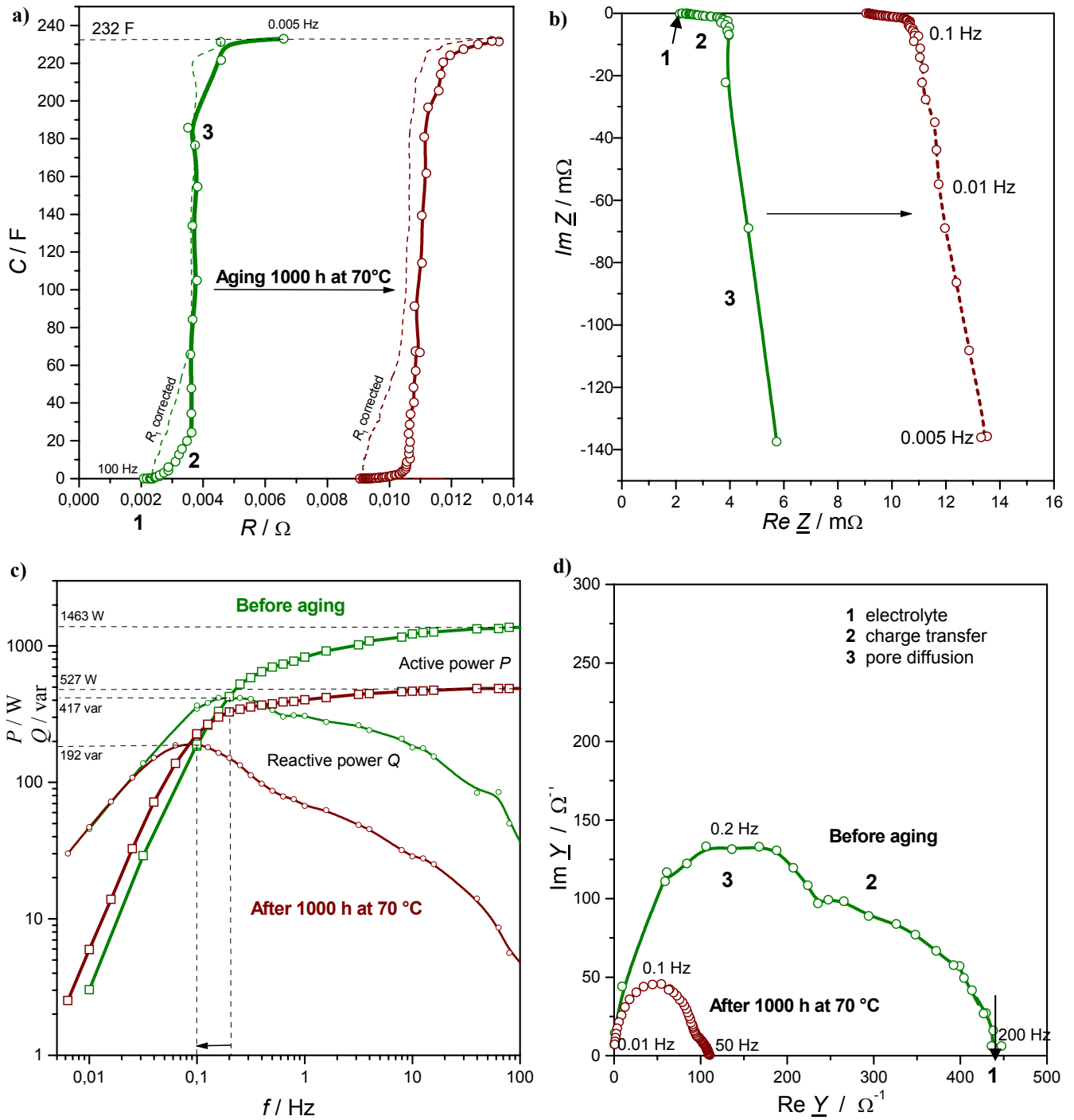


Fig. 15: Ageing of a MAXWELL supercapacitor (BCAP0350) at 1000 hours at 70°C. Impedance spectroscopy at 0 V reflects capacitance without faradaic reactions depending on voltage. Capacitance was calculated with respect to the equivalent circuit in Table 2c for a supercapacitor with negligible series resistance R_1 (some Milliohms), but not negligible leakage current resistance R_2 .

a) Capacitance versus resistance:

$$C(\omega) = \frac{\text{Im} \underline{Y}}{\omega} = \frac{-\text{Im} \underline{Z}}{\omega |\underline{Z}|^2} = \frac{-\text{Im} \underline{Z}}{\omega [(\text{Re} \underline{Z})^2 + (\text{Im} \underline{Z})^2]}$$

b) Complex plane plot of impedance

c) Ratio of reactive and active power ($U_0 = 2.5 \text{ V}$): $\eta = \frac{Q}{P}$

$$\begin{cases} Q = \text{Im} \left(\frac{1}{2} \underline{U} \underline{I}^* \right) = \frac{1}{2} U_0^2 \text{Im} \underline{Y} = -\frac{1}{2} U_0^2 \omega C \\ P = \text{Re} \left(\frac{1}{2} \underline{U} \underline{I}^* \right) = \frac{1}{2} U_0^2 \text{Re} \underline{Y} \end{cases}$$

d) Amittance (complex conductance):

$$\underline{Y} = \frac{1}{\underline{Z}} = \frac{\text{Re} \underline{Z}}{|\underline{Z}|^2} - j \frac{\text{Im} \underline{Z}}{|\underline{Z}|^2}$$

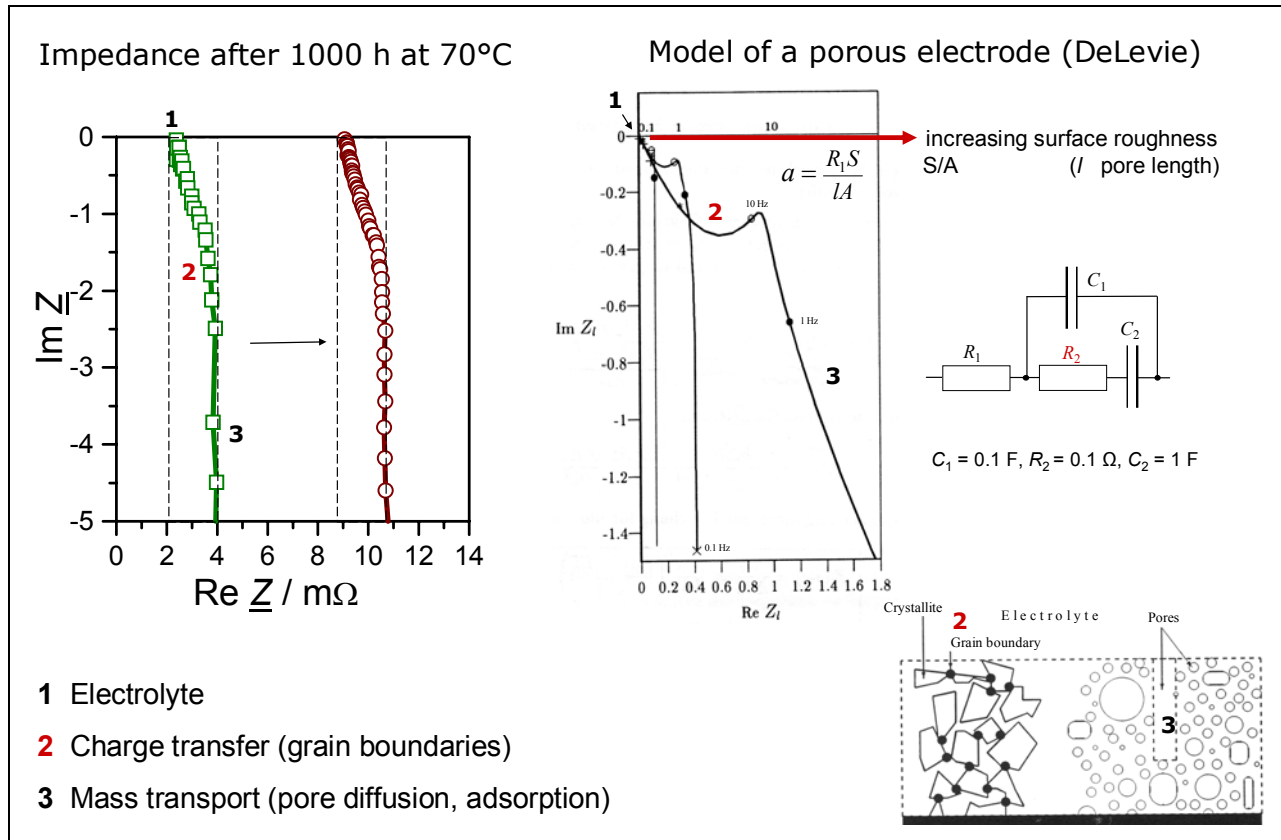


Fig. 16: Magnification of the high-frequency section in Figure 15 b). Explanation see Text and [8].

5.3 Leakage current

The leakage current – the residual current after 24 hours of charging at rated voltage (2.5 V) – increases markedly after a heat treatment.

- The unused Maxwell BCAP capacitor shows a leakage current of < 2 mA.
- The leakage current increases by a factor of eight after storing the capacitor at 70 °C for 1000 hours.

5.4 Selfdischarge

Self discharge in Figure 17 was measured at the fully charged capacitor. After a constant current charge over 24 hours without a protective resistance, the terminals were disconnected. The voltage across the capacitor was measured using a *dc* voltmeter with an internal resistance of >10 MΩ.

The selfdischarge voltage does not show an exponential but logarithmic decline: $U(t) = a - b \ln(c + t)$.

- After the thermal treatment at 70°C for 1000 hours, selfdischarge increased by a factor of 1.6 (relative to room temperature).
- The self-discharge current increases when the applied voltage is raised.

We estimated the *dc* resistance of selfdischarge by use of the time constant τ at 36,8 % of the rated voltage, and the capacitance found by impedance spectroscopy.

$$R_p = \frac{\tau}{C} = \frac{663,57 \cdot 3600 \text{ s}}{232 \text{ F}} = 10297 \Omega \text{ (at } 70 \text{ }^\circ\text{C)}$$

We observed – unfortunately not in every sample – a step in the self-discharge characteristics at 70°C after 640 to 900 hours, when the voltage drops under a limit of 1 V. This gives a hint at two interdependent selfdischarge processes. This might be an explanation why the Arrhenius diagram of *C* versus 1/*T* (in Kelvin) does not show a single straight line.

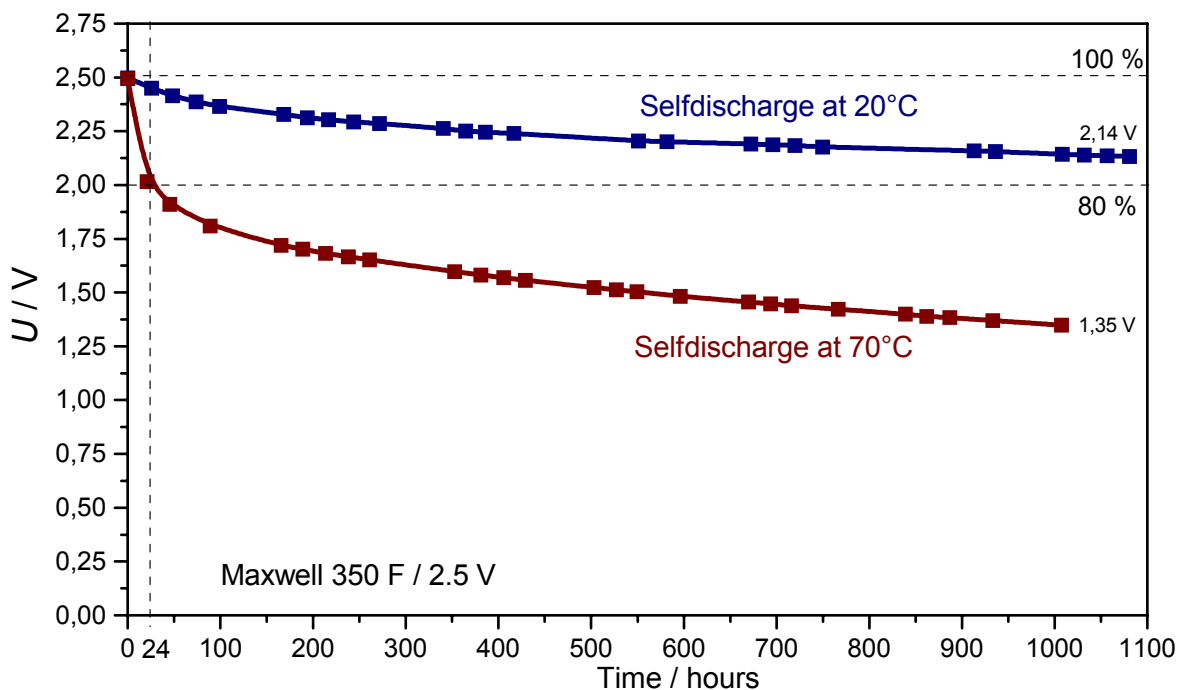


Fig. 17: Selfdischarge of a MAXWELL supercapacitor (BCAP0350)

6 References

- [1] a) P. KURZWEIL, H.-J. FISCHLE, Bipolar Supercapacitor For 42 V Applications, *Proc. 11th Int. Seminar on Double Layer Capacitors*, Deerfield Beach, USA, Dec. 3-5, 2001.
 b) P. KURZWEIL, H.-J. FISCHLE, Double-Layer Capacitor Development And Manufacture By HYDRA/AEG, *Proc. 13th Int. Seminar on Double Layer Capacitors*, Deerfield Beach, USA, Dec. 8-10, 2003, pp. 1-11.
- [2] a) P. KURZWEIL, G. DIETRICH, Double-layer capacitors for energy storage devices in space applications, *Proc. 2nd Int. Seminar on Double Layer Capacitors*, Deerfield Beach, USA, Dec. 8-10, 1992.
 b) P. KURZWEIL, O. SCHMID, High performance metal oxide supercapacitors, *Proc. 6th Int. Seminar on Double Layer Capacitors*, Deerfield Beach, USA, Dec. 9-11, 1996.
 c) P. KURZWEIL, O. SCHMID, Low temperature proton conducting metal oxide supercapacitor, *Meeting Abstracts*, The Electrochem. Soc. Fall Meeting, San Antonio, Texas, October 6-11 (1996) 825.
 d) see [3]
- [3] h) Double-layer capacitor, DE 43 13 474 A1 (1994); C2 (1997); DE 197 04 584 C2 (1999); US 5,930,108 (1999); EP 0 820 078 A1 (1998). Long time stable electrode, EP 0 622 815 B1 (1996). Electrode for an electrochemical cell, DE 196 40 926 C1 (1998).
- [3] P. KURZWEIL, O. SCHMID, A. LÖFFLER, Metal oxide supercapacitor for automotive applications, Replacement of starter batteries. *Proc. 7th Int. Seminar on Double Layer Capacitors*, Deerfield Beach, USA, Dec. 8-10, 1997.
- [4] EUCAR Traction Battery Working Group, Specification of test procedures for supercapacitors in electric vehicle application, September 1996.
- [5] P. KURZWEIL, H.-J. FISCHLE, The HYDRA Supercapacitor – Energy storage based on carbon and mixed metal oxides, *Proc. 12th Int. Seminar on Double Layer Capacitors*, Deerfield Beach, USA, Dec. 9-11, 2002.
- [6] P. KURZWEIL, Doppelschichtkondensatoren – Innovation auf Basis von Edelmetalloxiden, in: *Proc. 2nd Ulm Electrochemical Talks* (UECT), Ladungsspeicherung in der Doppelschicht, 20./21. June 1994, Universitätsverlag Ulm.
- [7] S. TRASATTI, P. KURZWEIL, *Platinum Metals Review* **38** (1994) 46-56.
- [8] a) IEC-40/1378 / DIN IEC 62391-1, Fixed electric double layer capacitors for use in electronic equipment. Part I: Generic specification, June 2004.
 b) IEC-40/1379 / DIN IEC 62391-2, Fixed electric double layer capacitors for use in electronic equipment. Part I: Sectional specification: Electric double layer capacitors for power application, June 2004.
- [9] P. KURZWEIL, Study on the ageing of supercapacitors based on acetonitrile, unpublished, 2005.
- [10] a) P. KURZWEIL *ac* Impedance Spectroscopy – A Powerful Tool For The Characterization Of Materials And Electrochemical Power Sources, *Proc. 14th Int. Seminar On Double Layer Capacitors*, Deerfield Beach, FL., U.S.A., December 6-8, 2004.
 b) P. KURZWEIL, H.-J. FISCHLE, A new monitoring method for electrochemical aggregates by impedance spectroscopy, *J. Power Sources* **127** (2004) 331-340.
- [11] R. DE LEVIE, Electrochemical response of porous and rough electrodes, in: T. Delahay (Ed.), *Advances in electrochemistry and electrochemical engineering*, Vol. 6, Interscience, New York 1967, p. 329-397.
- [12] a) E. HARZFELD, R. GALLAY, M. HAHN, R. KÖTZ, Presentation on Capacitance and series resistance determination in high power ultracapacitors, ESSCAP'04, Belfort, November 2004.
 b) R. KÖTZ, M. HAHN, R. GALLAY, Temperature Behaviour and Impedance Fundamentals of Supercapacitors, *UECT*, Ulm, 17-18 May 2004.
- [13] H. GUALOUS, R. GALLAY, *Technique de l'ingénieur*, D3335, to be published; ESSCAP'04, Belfort, November 2004.

Acknowledgement. – We thank U. BÄR for valuable measurements.